RSC Advances

PAPER

View Article Online
View Journal | View Issue

Cite this: *RSC Adv.*, 2019, **9**, 21202

Thermal and stress tension dual-responsive photonic crystal nanocomposite hydrogels

Dan Yan,[a] Wei Lu,[a] Lili Qiu,*[a] Zihui Meng*[a] and Yu Qiao[b]

Easily prepared dual-responsive optical nanocomposite hydrogel (ONH) sensors which are responsive to tension and temperature are reported in which polymethyl methacrylate (PMMA) colloidal arrays were embedded into the hydrogels to obtain an optical response. Because of the band gap in the photonic crystal (PhC), the bright color of ONHs can be tuned by an external stimulus according to Bragg's law. Thermosensitive *N*-isopropyl acrylamide (NiPAm) is added to the gel system, and by controlling NiPAm content and temperature, the contraction of the dual-response ONHs and the structural color response in the visible light range can change accordingly. Meanwhile, the temperature responses can be repeated more than seven times. Owing to the high biocompatibility, the excellent temperature response and the good mechanical strength of the ONHs, such optical biosensors have wide application in the biological field as an external stimulus sensor for implantable sensors, intracorporeal pressure measurement, and body temperature detection.

Received 12th April 2019
Accepted 15th June 2019

DOI: 10.1039/c9ra02768h

rsc.li/rsc-advances

Introduction

A photonic crystal (PhC) has a structure that generates an optical band gap due to periodic changes of the refractive index, and the band gap structure can modulate the propagation of light.[1–3] The repetitive structure of a PhC follows Bragg's diffraction law, enabling coverage of the entire visible spectrum and specified structural colors. Composite sensors fabricated by combining hydrogels with three-dimensional PhCs can respond to a variety of external chemical or physical stimulus, such as pH,[4,5] ionic strength,[6,7] electricity,[8,9] magnetic,[10,11] thermal[12–15] or mechanical stimulation.[16–18] Due to the unique optical properties of PhCs, PhC hydrogels have attracted considerable attention as response sensors.[19,20] In addition, the elastic polymer network and fluid-filled network space of the hydrogel are similar to that found in living systems.[21] Hydrogels have outstanding biocompatibility and hydrophilicity, so they have great potential in the field of biosensing and biomedicine.[22–26] However, their practical applications are severely limited by their poor mechanical properties and the high swelling rate of chemically cross-linked conventional organic polymer hydrogels (OPHs).

Nanocomposite hydrogels (NC gel) composed of a specific organic polymer and an inorganic water-soluble nanomaterial serving as a multifunctional cross-linker[27–29] can overcome most of the disadvantages of OPHs by their unique organic–inorganic network structure, and provide a variety of new properties.[30,31]

In a previous report,[32] we used *N*,*N*-dimethylacrylamide (DMAA, 99%) and acrylic acid (AA, 99%) as monomers to perform *in situ* radical copolymerization, and proposed a new type of ONH. Excellent mechanical properties can be obtained by using Al_2O_3 NPs as multifunctional cross-linkers in solution. The mechanical properties testing proves that the ONH has excellent mechanical strength and elasticity. PhC arrays were embedded into the hydrogels to obtain good optical performance. Due to the bandgap of three-dimensional PhC, the ONH can tune the structural color upon application of tension. In addition, the ONHs can also be used to detect pH changes in potassium dihydrogen phosphate (KDP) buffer visually. The excellent water stability, optical sensitivity to tension and pH, and biocompatibility of ONHs were demonstrated.

NiPAm polymer is a typical temperature-sensitive polymer with high temperature sensitivity and its lower critical solution temperature (LCST) is similar to body temperature. In this report, NiPAm was added to the original gel system to introduce a temperature responsive function to make the material have a wider range of application potentials, such as *in vivo* temperature or pH sensing, to achieve drug delivery and controlled release *in vivo*. By controlling NiPAm content and temperature, the contraction of the dual-response ONHs and the structural color response in the visible light range can change accordingly. As a potential implantable sensor, such materials have important implications for reducing patient injury and medical costs.

[a]*School of Chemistry and Chemical Engineering, Beijing Institute of Technology, Beijing, 102488, China. E-mail: qiulili@bit.edu.cn; mengzh@bit.edu.cn*
[b]*College of Mechanical and Materials Engineering, North China University of Technology, Beijing 100144, China*

Experimental

Fabrication of PMMA arrays

Monodisperse PMMA colloidal particles were prepared by using methods described previously.[32] Then, the three-dimensional (3D) PhC arrays were prepared by vertical self-assembly.[34]

Preparation of hydrogels

First, 1.7858 g Al_2O_3 colloidal solution (16.8%, $W_{Al_2O_3}/W_{water}$) was added into 20 mL beaker, and then 5 g ultrapure water was added under stirring. 1.1896 g DMAA, 0.2162 g AA and a certain amount of NiPAm were added into the beaker and allowed to continue to stir (200 rpm) for 20 min. Then the beaker was wrapped up with tin foil. After adding 0.015 g Irgacure, oxygen was removed by nitrogen bubbling for 15 min. After that, the PhC was filled by the prepared solution. Finally, the solution was crosslinked under UV light with a 365 nm UV light for 1 h. The obtained ONHs were then washed three times with ultrapure water (Scheme 1).[32]

Measurements and characterizations

The morphologies of the ONHs were characterized by scanning electron microscopy (SEM) and the color changes of the films were recorded by a digital camera at a constant angle.

Results and discussion

The SEM images of the PMMA colloidal array and ONH film are shown in Fig. 1. PMMA particles of 300 nm diameter were self-assembled into a 3D close-packed face-centered cubic (FCC) structure (Fig. 1(a)). The periodic structure was found to be well maintained after embedding inside the hydrogel matrix (Fig. 1(b)).

During the washing process after the reaction, the dual-responsive ONHs swelled because the unreacted monomers and cross-linkers inside the ONHs washed away. The mechanical strength of ONHs was obviously reduced and the adhesion was increased after adding NiPAm to the ONHs. The expansion of ONHs with NiPAm is about twice that of the ONHs without NiPAm. As shown in Fig. 2(b), the transparency of dual-ONHs decreased in the solution, the surface was slightly opaque and

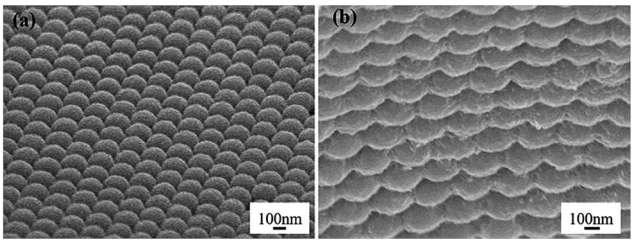

Fig. 1 SEM of (a) the PMMA colloidal array and (b) ONH film.

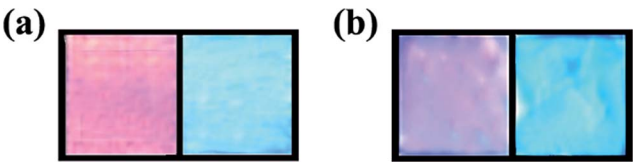

Fig. 2 The morphology of dual-responsive ONHs with the PhCs self-assembled by (a) 300 nm (left) and 180 nm (right) PMMA without NiPAm and (b) 300 nm (left) and 180 nm (right) PMMA with NiPAm.

the structural color of the PhC was slightly blurred, which is due to the shrinkage of the NiPAm polymer chain, but it becomes clear after removing from solution and it would not affect the subsequent observations.

Based on the preparation method, 1, 10, 25 and 50% NiPAm relative to the total gel prepolymerization solution was added, respectively. The dual-responsive gel film was cut into flakes, and ONHs of the same size without NiPAm (control group) were immersed in water or methanol–water (25/75, v/v) under different temperatures.

As shown in Fig. 3(a), 1% NiPAm addition in the dual-responsive ONHs did not change the temperature response of the gel. Meanwhile the samples swelled 7% along the length axis because the NiPAm occupied a certain number of double bonds on the ester, while diluting the gel prepolymer, reducing the degree of gel crosslinking, and making it easier to swell in the same environment. As the NiPAm content was increased to 10%, the dual-response OHNs showed a 14% shrinkage at the lengthwise axis in an aqueous environment at 32 °C. As the NiPAm level was increased to 50% the temperature range continued to expand. When the temperature was increased

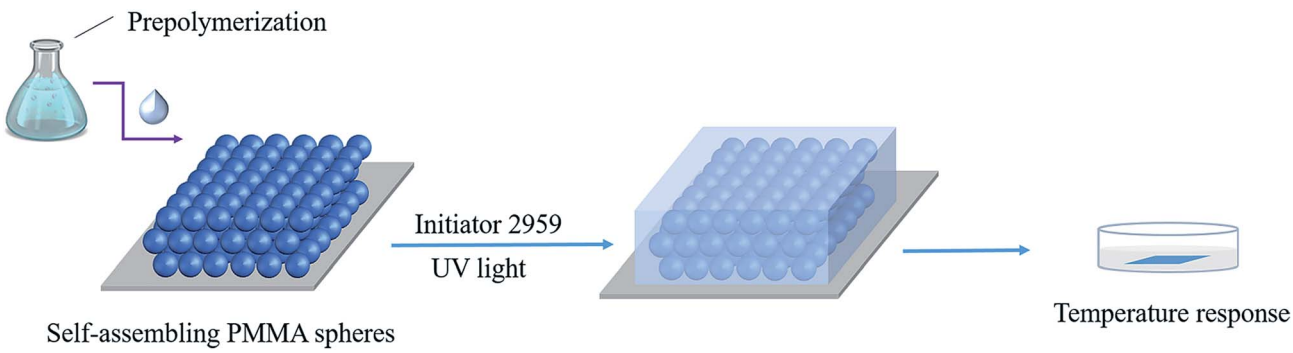

Scheme 1 Schematic illustration of ONH films.

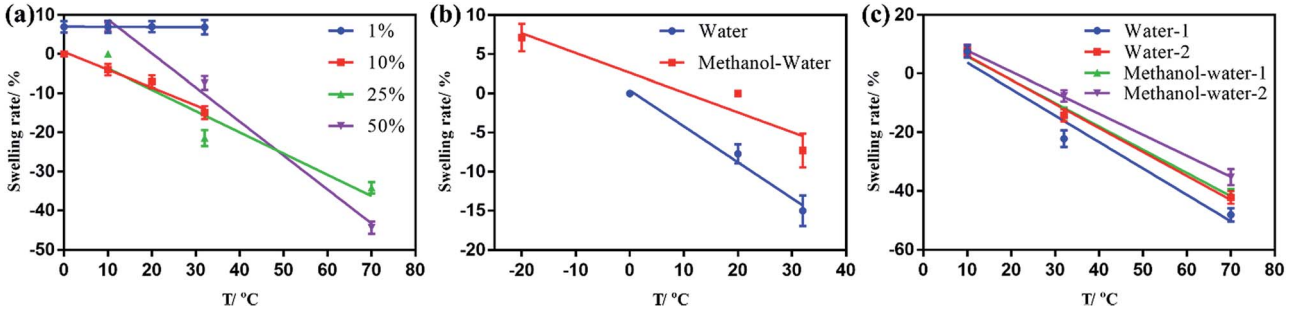

Fig. 3 (a) The relationship of swelling ratio and temperature of dual-responsive ONHs with 1, 10, 25 or 50% NiPAm addition; (b) the relationship of swelling ratio and temperature of dual-responsive ONHs with 10% of NiPAm addition in different environments; (c) the relationship of swelling ratio and temperature of dual-responsive ONHs with 50% NiPAm addition at different polymerization times.

from 32 to 70 °C, the shrinkage of the ONHs changed from 21.4% to about 50%. From the slopes of several lines in Fig. 3(a), the dual response PhC nanocomposite hydrogel with a high content of NiPAm was more sensitive to temperature, indicating higher NiPAm content led to more shrinkage of ONHs under the same conditions.

A certain amount of methanol was added into the solution to make the detection temperature drop below 0 °C in Fig. 3(b), and we can see that the presence of methanol affected the shrinkage of the gel compared to the pure water phase. Considering, for example, 10% NiPAm addition in the dual-responsive ONHs, the dual-response OHNs showed a 14% shrinkage for the lengthwise axis in an aqueous environment at 32 °C, compared to about 8% shrinkage in the lengthwise axis in methanol–water (25/75, v/v) solution. The dual-responsive ONHs with a high content of NiPAm addition are more sensitive to temperature in the water environment according to the slopes of the lines in Fig. 3(b).

The polymerization time of dual-responsive ONHs was adjusted from 1 to 2 h to observe its effect on the crosslinking of the gel (Fig. 3(c)). Comparing the dual-responsive ONHs with 50% of NiPAm addition polymerized for 1 and 2 h, increasing the polymerization time during preparation can reduce the swelling degree of the gel, with more than 7.1% extra shrinkage of the axial length of the 1 h sample under the same conditions. Therefore, when the content of NiPAm is 50% and the polymerization time is 1 h, the ONHs had the best sensitivity and the response range is from −20 to 70 °C. The temperature response range can be improved by changing the transition temperature of NiPAm by additives and comonomers.[33]

For a polymerization time of 1 h, and use of water immersion medium, the dual-responsive ONHs with 0, 25 and 50% NiPAm were immersed and then removed at 20, 60, 180 or 360 min, and the response at the axial length was measured. The kinetic response curve of dual-responsive ONHs was recorded and plotted at both 32 and 70 °C. The swelling is plotted as negative while the contraction is plotted as positive, and the test results are shown in Fig. 4.

It can be seen from the Fig. 4 that when the temperature is 32 °C, the ONHs without NiPAm showed a swelling effect in the complete deformation process, while ONHs with NiPAm contents of 25 and 50% produced different degrees of shrinkage.

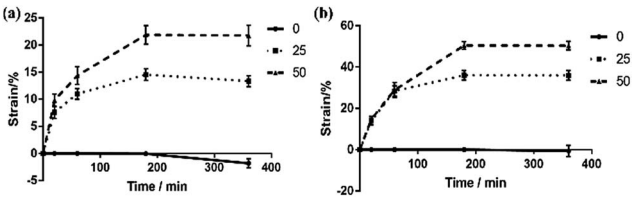

Fig. 4 Dynamic response curves of dual-response ONHs at (a) 32 °C and (b) 70 °C.

Deformation mainly occurred within the first hour and increased further with time, tending to stabilize when the immersion time reached 180 min. ONHs with NiPAm contents of 25 and 50% shrank by 14.28 and 21.85%, respectively, after this time corresponding to the experimental results in the previous sections. When the temperature was raised to 70 °C, the changes increased to 35% and 50%, respectively. Fig. 5 shows the response structural color of ONHs at 32 °C after different response times. The sizes and the colors of the gel patches before the response were similar, but different structural colors and shrinkages appeared after different response times. The shrinkage of the gel increased as the response time increased, so that the lattice spacing of the PhC decreased according to the Bragg diffraction formula, and as a result, the structural color changed, and the reflection peak was blue shifted. Since the shrinkage of the gel at different positions during varying times of immersion were different, the resultant films exhibited different colors. When the gel shrank to a stable state, the structural color of the film exhibited a single color, as shown in Fig. 5(c). Significant color changes could therefore be observed.

Taking the dual-response ONHs with the NiPAm content of 50% and the temperature of 70 °C as an example, the dual-

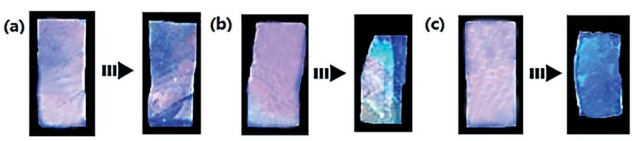

Fig. 5 Response structural color of NiPAm (25%) at 32 °C after immersion for (a) 5 min, (b) 20 min and (c) 180 min.

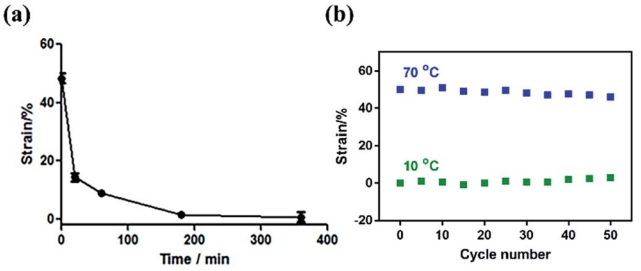

Fig. 6 (a) Resilience kinetic curves of dual-responsive ONHs in water at 10 °C and (b) reusability.

response ONHs polymerized for 1 h were immersed in a water bath at 10 °C. The recovery temperature response curve and the reusability were measured as shown in Fig. 6. ONHs can return to their original shape within 1 h. Under the above conditions, the dual-response ONHs can be reused more than 50 times.

Conclusions

In summary, we reported temperature and tension dual-responsive PhC nanocomposite hydrogel sensing materials. By adding NiPAm to the gel, the thermo-sensitivities of ONHs were obtained, and the tension/thermal dual response performance of gels was achieved. When the NiPAm content or temperature were increased, the contraction of the dual-response ONHs increased and the structural color change response in the visible light region changed accordingly, which is of great significance to further expand practical applications of such materials in the biomedical field as tension or temperature sensors.

Conflicts of interest

There are no conflicts to declare.

Acknowledgements

This work was supported by the National Natural Science Foundation of China (grant numbers U1530141, 21375009 and 21804009).

References

1 E. Yablonovitch, *Phys. Rev. Lett.*, 1987, **58**, 2059–2062.
2 D. Yan, L. L. Qiu, Y. F. Wang, *et al.*, *Chin. Chem. Lett.*, 2018, **29**, 922–926.
3 Y. J. Zhao, L. R. Shang, Y. Cheng, *et al.*, *Acc. Chem. Res.*, 2014, **47**, 3632–3642.
4 Y. W. Sun, Y. P. Zhang, J. J. Liu, *et al.*, *RSC Adv.*, 2016, **6**, 11204–11210.
5 W. P. Lustig, S. Mukherjee, N. D. Rudd, *et al.*, *Chem. Soc. Rev.*, 2017, **46**, 3242–3285.
6 M. S. Wang and Y. D. Yin, *J. Am. Chem. Soc.*, 2016, **138**, 6315–6323.
7 R. M. Parker, G. Guidetti, C. A. Williams, *et al.*, *Adv. Mater.*, 2018, **30**, 1704477.
8 M. Maldovan, *Nature*, 2013, **503**, 209–217.
9 P. Nagpal, D. P. Josephson, N. R. Denny, *et al.*, *J. Mater. Chem.*, 2011, **21**, 10836–10843.
10 I. Staude and J. Schilling, *Nat. Photonics*, 2017, **11**, 274–284.
11 J. D. Yin, S. C. Ruan, T. G. Liu, *et al.*, *Sens. Actuators, B*, 2017, **238**, 518–524.
12 N. Pourdavoud, S. Wang, A. Mayer, *et al.*, *Adv. Mater.*, 2017, **29**, 1605003.
13 P. N. Dyachenko, S. Molesky, A. Y. Petrov, *et al.*, *Nat. Commun.*, 2016, **7**, 11809.
14 H. H. Xing, J. Li, Y. Shi, *et al.*, *ACS Appl. Mater. Interfaces*, 2016, **8**, 9440–9445.
15 M. T. Barako, A. Sood, C. Zhang, *et al.*, *Nano Lett.*, 2016, **16**, 2754–2761.
16 M. A. Haque, T. Kurokawa, G. Kamita, *et al.*, *Chem. Mater.*, 2011, **23**, 5200–5207.
17 C. H. Liu, H. B. Ding, Z. Q. Wu, *et al.*, *Adv. Funct. Mater.*, 2016, **26**, 7937–7942.
18 W. Lee, D. Kim, S. Lee, *et al.*, *Nano Today*, 2018, **23**, 97–123.
19 C. I. Aguirre, E. Reguera and A. Stein, *Adv. Funct. Mater.*, 2010, **20**, 2565–2578.
20 J. A. Kelly, A. M. Shukaliak, C. C. Y. Cheung, *et al.*, *Angew. Chem., Int. Ed.*, 2013, **52**, 8912–8916.
21 J. Wang, G. P. Chen, Z. Zhao, *et al.*, *Sci. China Mater.*, 2018, **61**, 1314–1324.
22 M. Maity, V. S. Sajisha, U. Maitra, *et al.*, *RSC Adv.*, 2015, **5**, 90712–90719.
23 J. Li, L. T. Mo, C. H. Lu, *et al.*, *Chem. Soc. Rev.*, 2016, **45**, 1410–1431.
24 Z. Cai, N. L. Smith, J. Zhang, *et al.*, *Anal. Chem.*, 2015, **87**, 5013–5025.
25 S. Kim, J. Mitropoulos, H. T. Spitzberg, *et al.*, *Nat. Photonics*, 2012, **6**, 817–822.
26 Z. Cai, J. Zhang, F. Xue, *et al.*, *Anal. Chem.*, 2014, **86**, 4840–4847.
27 M. Takafuji, S. Yamada and H. Ihara, *Chem. Commun.*, 2011, **47**, 1024–1026.
28 Y. Wu, M. Xia, Q. Fan, *et al.*, *Chem. Commun.*, 2010, **46**, 7790–7792.
29 Z. Wang, J. Zhang, J. Xie, *et al.*, *Adv. Funct. Mater.*, 2010, **20**, 3784–3790.
30 S. Goenka, V. Sant and S. Sant, *J. Controlled Release*, 2014, **173**, 75–88.
31 K. Wang, X. Zhang, X. Y. Sun, *et al.*, *Sci. China Mater.*, 2016, **59**, 412–420.
32 L. Wei, H. J. Li, B. Huo, *et al.*, *Sens. Actuators, B*, 2016, **234**, 527–533.
33 C. Ayoung, Y. Jeonghee, S. Ravi, *et al.*, *NPG Asia Mater.*, 2018, **10**, 912–922.
34 Z. Q. Yan, M. Xue, Q. He, *et al.*, *Anal. Bioanal. Chem.*, 2016, **408**, 8317–8323.